Robotica (2002) volume 20, pp. 367–374. © 2002 Cambridge University Press
DOI: 10.1017/S0263574702004101 Printed in the United Kingdom

Simultaneous base and tool calibration for self-calibrated parallel robots

Guilin Yang*, I-Ming Chen†, Song Huat Yeo† and Wee Kiat Lim‡

(Received in Final Form: January 9, 2002)

SUMMARY

In this paper, we focus on the base and tool calibration of a self-calibrated parallel robot. After the self-calibration of a parellel robot by using the built-in sensors in the passive joints, its kinematic transformation from the robot base to the mobile platform frame can be computed with sufficient accuracy. The base and tool calibration, hence, is to identify the kinematic errors in the fixed transformations from the world frame to the robot base frame and from the mobile platform frame to the tool (end-effector) frame in order to improve the absolute positioning accuracy of the robot. Using the mathematical tools from group theory and differential geometry, a simultaneous base and tool calibration model is formulated. Since the kinematic errors in a kinematic transformation can be represented by a twist, i.e. an element of $se(3)$, the resultant calibration model is simple, explicit and geometrically meaningful. A least-square algorithm is employed to iteratively identify the error parameters. The simulation example shows that all the preset kinematic errors can be fully recovered within three to four iterations.

KEYWORDS: Parallel robots; Base-tool calibration; Special Euclidean group; Lie algebra.

1. INTRODUCTION

A parallel robot is a closed-loop mechanism in which the mobile platform is connected to the base by at least two serial kinematic chains (legs). Because a parallel robot usually has a limited workspace, trajectory planning and application development become difficult. In our research, we employ the modularity concept in the design of parallel robot configurations for precision assembly and light machining tasks. The modularly designed parallel robot system consists of a collection of individual actuator modules, passive joint modules, rigid links (connectors), and mobile platforms. A modular parallel robot configuration thus can be rapidly constructed and deployed for a specific task.[1]

One of the main concerns in the modular robot system is the positioning accuracy of the robot end-effector. A set of robot modules are joined together to form a complete parallel robot assembly. Factors like machining tolerance, compliance, and wear of the connecting mechanism will affect the positioning accuracy of the robot. Especially, the assembly errors of a modular robot are usually larger than those of a robot having fixed configuration. Hence, identifying the critical kinematic parameters to improve the positioning accuracy of the robot becomes a very important issue for modular reconfigurable parallel robots.

Because of the closed-loop structure of a parallel robot, its kinematic calibration can be divided into two subsequent procedures: (1) *Self-calibration*; and (2) *Base and tool calibration*. The purpose of self-calibration is to calibrate the closed-loop mechanism itself by using the built-in sensors in the passive joints. After the self-calibration of the robot, in general, the kinematic transformation from the robot base to the mobile platform can be computed with sufficient accuracy. The base and tool calibration, on the other hand, is to identify the fixed kinematic transformations from the world frame to robot base frame and from the mobile platform frame to the end-effector frame by using external measuring equipment. Apparently, the base and tool calibration is aimed at improving the absolute positioning accuracy of the robot.

Past research efforts on parallel robot calibration have been concentrated on the self-calibration techniques. A number of self-calibration algorithms have been developed.[2–6] Based on the product-of-exponentials (POE) formula, a geometric self-calibration model has also been proposed by the authors.[7] On the other hand, the base and tool calibration of a parallel robot is similar to that of a serial type robot, and there is much work addressing such a calibration issue. Zhuang[8] et al. based on the quaternion algebra, propose a linear solution that allows the simultaneous computation of these two kinematic transformations. This approach is non-iterative and fast. However, this linear method has the formulation singularity problem such that some arrangements of robot world frame and robot base frame have to be avoided. Another inconvenience of this approach is that the geometric parameters are estimated in a two-stage process so that the estimation errors from the first stage will propagate to the second stage. It will be always the case when noise and measurement errors exist. Other recent works related to the base and tool calibration can be found in Park and Martin[9] and Dornaika and Horaud.[10]

Different from the linear solution approach, we cast the base and tool calibration problem into an iterative parameter identification process. The reason behind this is that although the linear (closed-form) solution approach, in principle, is computationally efficient, it becomes ineffective in the presence of noise and measurement errors. Using

* Automation Technology Division, Gintic Institute of Manufacturing Technology (Singapore), 638075.
† School of Mechanical & Production Engineering, Nanyang Technological University (Singapore), 639798.
‡ DSO National Laboratories (Singapore), 118230.

https://doi.org/10.1017/S0263574702004101 Published online by Cambridge University Press

the mathematical tools from differential geometry and group theory, a simple and explicit base and tool calibration algorithm is formulated in this paper. The basic idea of this algorithm is that the kinematic errors in a fixed kinematic transformation can be represented by a twist, i.e. an element of of $se(3)$. Because a twist also has a 6-dimensional vector representation, the formulation is significantly simplified. Besides, it does not suffer from any formulation singularity problem and is generous enough to allow very large kinematic errors. The simulation examples show that it is also computational efficient as all the preset kinematic errors can be fully recovered within three to four iterations.

The remaining sections of this article are organized as follows. Section 2 briefly introduces some fundamental geometric concepts pertaining to the formulation of the base and tool calibration model. The formulation of the base and tool calibration model for a self-calibrated parallel robot is addressed in Section 3. A computer simulation example for calibrating a 6-DOF, 3RRRS-type parallel robot is then presented in Section 4. This paper is summarized in Section 5.

2. GEOMETRIC BACKGROUND

In this section, some fundamental geometric concepts pertaining to the formulation of the base and tool calibration model are briefly recalled (please refer to references 11 to 14 for more details).

In robot kinematics, it is sufficient to think of $SE(3)$, the *Special Euclidean Group* of rigid body motions, as consisting of matrices of the form

$$\begin{bmatrix} R & p \\ 0 & 1 \end{bmatrix} \tag{1}$$

where $R \in SO(3)$ is interpreted as a rigid body rotation and $p \in \Re^{3\times 1}$ as a rigid body translation. Here, $SO(3)$, the *Special Orthogonal Group*, denotes the group of 3×3 rotation matrices. Elements of $SE(3)$ can also be denoted by the ordered pair (p, R), with group multiplication understood to be $(p_1, R_1).(p_2, R_2) = (R_1 p_2 + p_1, R_1 R_2)$. $SE(3)$ is a Lie group of dimension six.

The *Lie algebra* of $SE(3)$, denoted $se(3)$, consists of matrices of the form

$$\begin{bmatrix} \hat{w} & v \\ 0 & 0 \end{bmatrix} \tag{2}$$

where

$$\hat{w} = \begin{bmatrix} 0 & -w_z & w_y \\ w_z & 0 & -w_x \\ -w_y & w_x & 0 \end{bmatrix} \tag{3}$$

The set of 3×3 real skew-symmetric matrices, $\hat{w}$, forms the Lie algebra of $SO(3)$, denoted by $so(3)$. Note that an element of $\hat{w} \in so(3)$ can also be regarded as a vector $w \in \Re^{3\times 1}$. An element of $se(3)$ will thus admit a 6×1 vector presentation: $(v, w) \in \Re^{6\times 1}$, termed a twist. The twist represents the line coordinate of the *screw* axis of a general rigid body motion, in which w and v are the direction and position vectors of the screw axis, respectively.

On matrix Lie algebras, the *Lie bracket* is given by the matrix commutator: if A and B are elements of a matrix Lie algebra, then $[A, B] = AB - BA$. In particular, on $so(3)$ the Lie bracket of two elements corresponds to their vector product: $[w_1, w_2] = w_1 \times w_2$. On $se(3)$, the Lie bracket of two elements (v_1, w_2) and (v_2, w_2) is given by

$$[(v_1, w_1), (v_2, w_2)] = (w_1 \times v_2 - w_2 \times v_1, w_1 \times w_2). \tag{4}$$

An element of a Lie group can also be identified with a linear mapping between its Lie algebra via the *adjoint representation*. Suppose G is a matrix Lie group with Lie algebra g. For every $X \in G$ the adjoint map $Ad_X : g \to g$ is defined by $Ad_X(x) = XxX^{-1}$ for $x \in g$. If $X = (p, R)$ is an element of $SE(3)$, then its adjoint map acting on an element $x = (v, w)$ of $se(3)$ is given by

$$Ad_X(x) = (p \times Rw + Rv, Rw) \tag{5}$$

which also admits the 6×6 matrix representation

$$Ad_X(x) = \begin{bmatrix} R & \hat{p}R \\ 0 & R \end{bmatrix} . \begin{bmatrix} v \\ w \end{bmatrix} \tag{6}$$

It can be readily verified that $Ad_X^{-1} = Ad_{X-1}$ and $Ad_X Ad_X = Ad_{XY}$ for any $X, Y \in SE(3)$.

An important connection between a Lie group, $SE(3)$, and its Lie algebra, $se(3)$, is the exponential mapping, defined on each Lie algebra. Let $\hat{s} \in se(3)$ $(s = (v, w))$, and $\|w\|^2 = w_x^2 + w_y^2 + w_z^2$, then:

$$e^{\hat{s}} = \begin{bmatrix} e^{\hat{w}} & Av \\ 0 & 1 \end{bmatrix} \in SE(3) \tag{7}$$

where

$$e^{\hat{w}} = I + \frac{\sin\|w\|}{\|w\|}\hat{w} + \frac{1-\cos\|w\|}{\|w\|^2}\hat{w}^2$$

$$A = I + \frac{1-\cos\|w\|}{\|w\|^2}\hat{w} + \frac{\|w\| - \sin\|w\|}{\|w\|^3}\hat{w}^2$$

The matrix logarithm also establishes a connection between a Lie group and its Lie algebra while the Lie group is in the neighborhood of the identity. Let $R \in SO(3)$ such that trace $\neq -1, 1 + 2\cos\phi = \text{trace}(R)$, and $\|\phi\| < \pi$, then

$$\log \begin{bmatrix} R & p \\ 0 & 1 \end{bmatrix} = \begin{bmatrix} \hat{w} & A^* p \\ 0 & 0 \end{bmatrix} \in se(3) \tag{8}$$

https://doi.org/10.1017/S0263574702004101 Published online by Cambridge University Press

where:

$$\hat{w} = \log R = \frac{\phi}{2 \sin \phi}(R - R^T)$$

$$A^* = I - \frac{1}{2}\hat{w} + \frac{2 \sin \|w\| - \|w\|(1 + \cos \|w\|)}{2 \|w\|^2 \sin \|w\|}\hat{w}^2$$

If ϕ is very small, $\hat{w} \approx (R - R^T)/2$.

3. BASE AND TOOL CALIBRATION MODEL

3.1. Basic Considerations

Once a parallel robot is self-calibrated, as shown in Fig. 1, the forward kinematic transformation from the robot base frame B to the mobile platform frame A can be computed precisely when the actuator joint angles are known. Hence, the base and tool calibration is to identify the kinematic errors in the fixed transformations from the robot world frame $B0$ to robot base frame B and from the mobile platform frame A to the tool (end-effector) frame E.

3.2. Calibration Model

Now let us first consider the kinematic transformation from the robot base frame $B0$ to the end-effector frame E. As shown in Fig. 1, this forward kinematic transformation, $T_{B0,E}(q)$, can be given by:

$$T_{B0,E}(q) = T_{B0,B} T_{B,A}(q) T_{A,E} \tag{9}$$

where $T_{B0,B}$ and $T_{A,E}$ are the fixed kinematic transformations from the robot world frame $B0$ to the robot base frame B and from the mobile platform frame A to the tool frame E respectively. Since $T_{B,A}(q)$ is the forward kinematic transformation of the self-calibrated parallel robot, we can assume that $T_{B,A}(q)$ is error-free and can be computed with sufficient accuracy. The kinematic errors will only come from the fixed kinematic transformations $T_{B0,B}$ and $T_{A,E}$.

According to the definition of matrix logarithm defined on $SE(3)$, there exists at least a $\hat{t} \in se(3)$ for a given $T \in SE(3)$, such that $e^{\hat{t}} = T$. Hence, it is sufficient to let $e^{\hat{t}_{B0,B}} = T_{B0,B}$ and $e^{\hat{t}_{A,E}} = T_{A,E}$, where $\hat{t}_{B0,B}$, $\hat{t}_{A,E} \in se(3)$. Equation (9) can be rewritten as:

$$T_{B_0,E}(q) = e^{\hat{t}_{B0,B}} T_{B,A}(q) e^{\hat{t}_{A,E}} \tag{10}$$

Now we assume that the kinematic errors occur only in $T_{B0,B}$ and $T_{A,E}$, hence in $\hat{t}_{B0,B}$ and $\hat{t}_{A,E}$. Let the kinematic errors in $\hat{t}_{B0,B}$ be expressed in the robot world frame B_0, denoted by $\delta\hat{t}_{B0,B}$, and $\hat{t}_{A,E}$ be expressed in the mobile platform frame A, denoted by $\delta\hat{t}_{A,E}$. Since both $\hat{t}_{B0,B}$ and $\hat{t}_{A,E}$ belong to $se(3)$, $\delta\hat{t}_{B0,B}$ and $\delta\hat{t}_{A,E}$ will belong to $se(3)$. Also we have, $\delta e^{\hat{t}_{B0,B}} = \delta\hat{t}_{B0,B} e^{\hat{t}_{B0,B}}$ and $\delta e^{\hat{t}_{A,E}} = \delta\hat{t}_{A,E} e^{\hat{t}_{A,E}}$. Linearizing Equation (9) with respect to $\hat{t}_{B0,B}$ and $\hat{t}_{A,E}$, we have

$$\begin{aligned}\delta T_{B0,E}(q) = {} & \delta\hat{t}_{B0,B} e^{\hat{t}_{B0,B}} T_{B,A}(q) e^{\hat{t}_{A,E}} \\ & + e^{\hat{t}_{B0,B}} T_{B,A}(q) \delta\hat{t}_{A,E} e^{\hat{t}_{A,E}}\end{aligned} \tag{11}$$

Right-multiplicating both sides of Equation (11) with $T^{-1}_{B0,E}(q)$, we get:

$$\begin{aligned}&\delta T_{B0,E}(q) T^{-1}_{B0,E}(q) = \\ &\quad \delta\hat{t}_{B0,B} + T_{B0,A}(q)\, \delta\hat{t}_{A,E}\, T^{-1}_{B0,A}(q)\end{aligned} \tag{12}$$

where:

$$\begin{aligned}&T_{B0,A}(q) = T_{B0,B} T_{B,A}(q), \\ &\delta T_{B0,E}(q) T^{-1}_{B0,E}(q) \approx T^{a}_{B0,E}(q) T^{-1}_{B0,E}(q) - I_{4\times4}.\end{aligned}$$

Here, $T^{a}_{B0,E}(q)$ is the actual (measured) end-effector pose. Based on the definition of the *matrix logarithm* and the *adjoint representation* on $SE(3)$, we have:

$$\begin{aligned}&\log [T^{a}_{B0,E}(q) T^{-1}_{B0,E}(q)] \approx T^{a}_{B0,E}(q) T^{-1}_{B0,E}(q) - I_{4\times4} \\ &T_{B0,A}(q)\, \delta\hat{t}_{A,E}\, T^{-1}_{B0,A}(q) = Ad_{T_{B0,A}(q)}\, \delta\hat{t}_{A,E}\end{aligned}$$

Hence, Equation (12) can be rewritten as:

$$\begin{aligned}&\log [T^{a}_{B0,E}(q) T^{-1}_{B0,E}(q)]^{V} \\ &= \delta t_{B0,B} + Ad_{T_{B0,A}(q)}\, \delta t_{A,E}\end{aligned} \tag{13}$$

where $\log [T^{a}_{B0,E}(q) T^{-1}_{B0,E}(q)]^{V} \in \Re^{6\times1}$ is the vector representation of $\log [T^{a}_{B0,E}(q) T^{-1}_{B0,E}(q)]^{V} \in se(3)$. Similarly, $\delta t_{B0,B}$ and $\delta t_{A,E}$ are the 6-dimensional vector representations of $\hat{\delta} t_{B0,B} \in se(3)$ and $\hat{\delta} t_{A,E} \in se(3)$, respectively.

Geometrically, $\log [T^{a}_{B0,E}(q) T^{-1}_{B0,E}(q)]^{V}$ represents the gross kinematic error of the toolframe expressed in the robot world frame. From Equation (13), it is equal to the sum of the kinematic errors in $T_{B0,B}$ and $T_{A,E}$ expressed in the robot world frame, i.e. the sum of the word frame representation of $\delta t_{B0,B}$ and $\delta t_{A,E}$. Note that, in each of the 6-dimensional error vectors $\delta t_{B0,B}$ and $\delta t_{A,E}$, the first three parameters represent the position errors (δx, δy, and δz), while the last three parameters represent the orientation errors ($\delta\alpha_x$, $\delta\beta_y$, and $\delta\gamma_z$). A detailed geometrical description of these parameters can be found in the following subsection. Equation (13) can also be further simplified as the following linear calibration model:

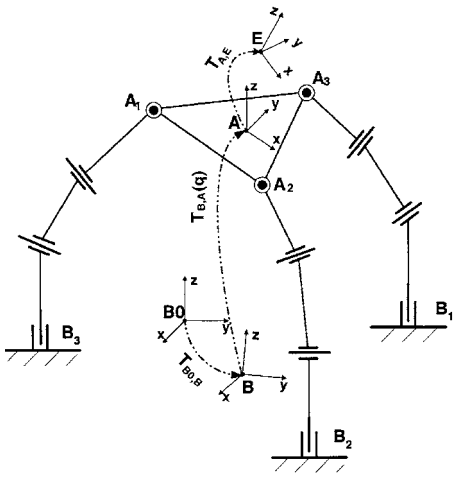


Fig. 1. Coordinate frames for base and tool calibration.

https://doi.org/10.1017/S0263574702004101 Published online by Cambridge University Press

$$y = Jx \tag{14}$$

where:

$$y = \log\left[T^{a}_{B0,E}(q)\, T^{-1}_{B0,E}(q)\right]^{V}(\cdot) \in \Re^{6\times 1}$$

$$J = \left[I_{6\times 6}\, Ad_{T_{B0,A}}(q)\right] \in \Re^{6\times 12}$$

$$x = \begin{bmatrix} \delta t_{B0,B} \\ \delta t_{A,E} \end{bmatrix} \in \Re^{12\times 1}$$

In Equation (14), we totally have 12 parameters to be identified, which can reflect kinematic errors existed in the whole system.

3.3. Geometrical Description of the Kinematic Errors

As shown in Fig. 2, let $T_{i-1,i}$ be the fixed kinematic transformation from frame $i-1$ to frame i. However, because of the geometric errors in the dyad, the nominal frame i will be different from its actual counterpart, denoted by frame i^a.

Based on the differential transformation principle[15,16], the nominal frame i ($T_{i-1,i}$) can be kinematically transformed into frame i^a ($T^{a}_{i-1,i}$) under an infinitesimal translation **Trans** (δx_{i-1}, δy_{i-1}, δz_{i-1}) followed by an infinitesimal rotation, **Rot** ($\delta\alpha_{i-1}$, $\delta\beta_{i-1}$, $\delta\gamma_{i-1}$), where δx_{i-1}, δy_{i-1}, and δz_{i-1} are infinitesimal displacements along x, y, and z-axis of frame $i-1$ respectively, and $\delta\alpha_{i-1}$, $\delta\beta_{i-1}$, and $\delta\gamma_{i-1}$ are infinitesimal angles about x, y, and z-axis of frame $i-1$ respectively. Then

$$\begin{aligned} T^{a}_{i-1,i} = {} & \mathbf{Trans}(\delta x_{i-1}, \delta y_{i-1}, \delta z_{i-1}). \\ & \mathbf{Rot}(\delta\alpha_{i-1}, \delta\beta_{i-1}, \delta\gamma_{i-1}).\, T_{i-1,i}(0). \end{aligned} \tag{15}$$

Note that the differential transformation is expressed in frame $i-1$. Hence, Equation (15) follows the left multiplicative differential transformation of $T_{i-1,i}$.[15,16]

Based on the definition of the differential transformation, we have

$$\mathbf{Trans}(\delta x_{i-1}, \delta y_{i-1}, \delta z_{i-1}) = \begin{bmatrix} 1 & 0 & 0 & \delta x_{i-1} \\ 0 & 1 & 0 & \delta y_{i-1} \\ 0 & 0 & 1 & \delta z_{i-1} \\ 0 & 0 & 0 & 1 \end{bmatrix} \tag{16}$$

$$\mathbf{Rot}(\delta\alpha_{i-1}, \delta\beta_{i-1}, \delta\gamma_{i-1}) = \begin{bmatrix} 1 & -\delta\gamma_{i-1} & \delta\beta_{i-1} & 0 \\ \delta\gamma_{i-1} & 1 & -\delta\alpha_{i-1} & 0 \\ -\delta\beta_{i-1} & \delta\alpha_{i-1} & 1 & 0 \\ 0 & 0 & 0 & 1 \end{bmatrix} \tag{17}$$

Because the geometric errors are very small, the differential change of frame i, denoted by $\delta T_{i-1,i}$, can be approximately given by:

$$\delta T_{i-1,i} \approx T^{a}_{i-1,i} - T_{i-1,i}. \tag{18}$$

Note that $\delta T_{i-1,i}$ in Equation (18) is also expressed in frame $i-1$.

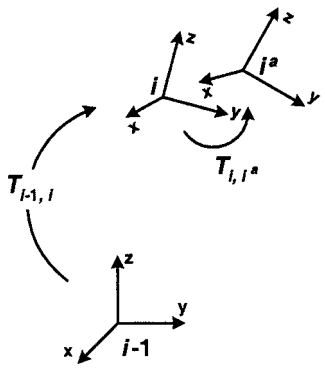


Fig. 2. Geometric errors in a kinematic transformation.

Substituting Equations (16), (17), and (15) into Equation (18), we get:

$$\begin{aligned} \delta T_{i-1,i} = {} & [\,\mathbf{Trans}(\delta x_{i-1}, \delta y_{i-1}, \delta z_{i-1}). \\ & \mathbf{Rot}(\delta\alpha_{i-1}, \delta\beta_{i-1}, \delta\gamma_{i-1}) - I_{4\times 4}].\, T_{i-1,i} \end{aligned} \tag{19}$$

$$= \delta\hat{t}_{i-1,i}\,.\,T_{i-1,i} \tag{20}$$

where $I_{4\times 4}$ represents the 4×4 identity matrix; and:

$$\begin{aligned} \delta\hat{t}_{i-1,i} = {} & [\mathbf{Trans}(\delta x_{i-1}, \delta y_{i-1}, \delta z_{i-1}. \\ & \mathbf{Rot}(\delta\alpha_{i-1}, \delta\beta_{i-1}, \delta\gamma_{i-1}) - I_{4\times 4}] = \\ & \begin{bmatrix} 0 & -\delta\gamma_{i-1} & \delta\beta_{i-1} & \delta x_{i-1} \\ \delta\gamma_{i-1} & 0 & -\delta\alpha_{i-1} & \delta y_{i-1} \\ -\delta\gamma_{i-1} & \delta\alpha_{i-1} & 0 & \delta z_{i-1} \\ 0 & 0 & 0 & 0 \end{bmatrix} \end{aligned} \tag{21}$$

In Equation (21), $\delta\hat{t}_{i-1,i}$ can represent the geometrical error in the fixed kinematic transformation $T_{i-1,i}$, observed in frame $i-1$. It is apparent that $\delta\hat{t}_{i-1,i}$ is an element of $se(3)$, and hence can be identified by a 6×1 vector such that $\delta\hat{t}_{i-1,i} \rightarrow \delta t_{i-1,i} = (\delta x_{i-1}, \delta y_{i-1}, \delta z_{i-1}, \delta\alpha_{i-1}, \delta\beta_{i-1}, \delta\gamma_{i-1})^{T}$. Equation (20) also implies that:

$$\delta\hat{t}_{i-1,i} = \delta T_{i-1,i}\, T^{-1}_{i-1,i} \tag{22}$$

From the above discussion, it can be concluded that the geometric errors in a kinematic transformation or a frame can be uniformly represented by a twist, i.e. an element of $se(3)$. With such a geometrical treatment, the formulation of the calibration model can be systematically simplified.

3.4. An Iterative Least-Square Algorithm

Based on the calibration model Equation (14), an iterative least-square algorithm is employed for the calibration solution. To obtain reliable calibration result, we usually need to measure the end-effector poses in a number of different robot postures. Suppose we need to take m sets of measured data. For i^{th} measurement, we can obtain a $y_{[i]}$ as well as an identification Jacobian matrix $J_{[i]}$. After m measurements, we can stack $y_{[i]}$ and $J_{[i]}$ to form the following equation:

$$\tilde{y} = \tilde{J}x \tag{23}$$

https://doi.org/10.1017/S0263574702004101 Published online by Cambridge University Press

where:

$$\tilde{y} = \begin{bmatrix} y_{[1]} \\ y_{[2]} \\ \vdots \\ y_{[m]} \end{bmatrix} \in \Re^{6m\times 1}, \tilde{\mathrm{J}} = \begin{bmatrix} J_{[1]} \\ J_{[2]} \\ \vdots \\ J_{[m]} \end{bmatrix} \in \Re^{6m\times 12},$$

$$x = \begin{bmatrix} \delta t_{B0,B} \\ \delta t_{A,E} \end{bmatrix} \in \Re^{12\times 1}$$

Since Equation (23) consists of $6m$ linear equations with 12 variables (normally $m>2$), the linear least squares algorithm is employed for the parameter identification. The least-square solution of x is given by

$$x = (\tilde{J}^T \tilde{J})^{-1} \tilde{J}^T \tilde{Y} \tag{24}$$

where $(\tilde{J}^T \tilde{J})^{-1} \tilde{J}^T$ is the pseudoinverse of $\tilde{J}$.
The solution of Equation (24) can be further improved through iterative substitution as shown in Fig. 3. Once the kinematic error parameter vector, x is identified, $T_{B0,B}$ and $T_{A,E}$ are updated by substituting x into the following equations:

$$\begin{aligned} T^{new}_{B0,B} &= e^{\delta\hat{i}B0,B} T^{old}_{B0,B} \\ T^{new}_{A,E} &= e^{\delta\hat{i}A,E} T^{old}_{A,E} \end{aligned} \tag{25}$$

The same procedure is repeated until the norm of the error vector, $||x||$, approaches zero. Then the final $T_{B0,B}$ and $T_{A,E}$, represent the calibrated kinematic transformations, denoted by $T^c_{B0,B}$ and $T^c_{A,E}$ respectively.

Note that the kinematic error vector, x, will no longer represent the actual kinematic errors after iterations. However, the actual kinematic errors can be extracted by using the matrix logarithm to compare the calibrated frame poses with their nominal counterparts such that:

$$\begin{aligned} \delta t_{B0,B} &= \log [T^c_{B0,B}(0) T^{-1}_{B0,B}(0)]^V \\ \delta t_{A,E} &= \log [T^c_{A,E}(0) T^{-1}_{A,E}(0)]^V \end{aligned} \tag{26}$$

After calibration, the forward kinematic equation becomes

$$T^c_{B0,E}(q) = T^c_{B0,B} T_{B,A}(q) T^c_{A,E} \tag{27}$$

In order to evaluate the calibration result, we define the deviation metrics between the measured (actual) 'a' and calibrated 'c' end-effector (tool) frames mathematically as

$$\delta R = \frac{1}{m} \sum_{i=1}^{m} || \log (R_{ai}^{-1} R_{ci})^V || \tag{28}$$

$$\delta P = \frac{1}{m} \sum_{i=1}^{m} ||P_{ai} - P_{ci}|| \tag{29}$$

where δR and δP denote the average quantified orientation and position deviations between the calibrated and actual poses, respectively.

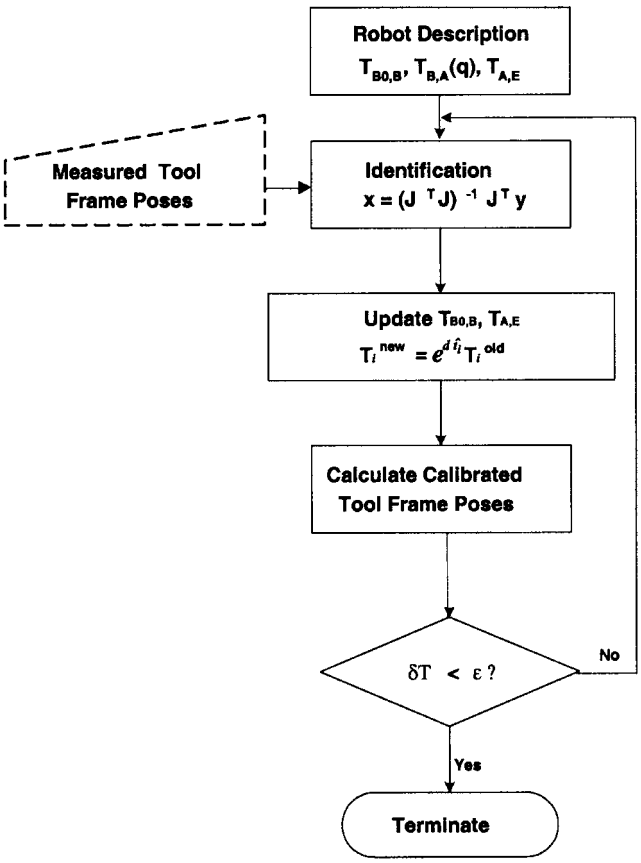


Fig. 3. Iterative calibration loop.

4. COMPUTER SIMULATION

In this section, a base and tool calibration example for a self-calibrated 3-legged (6-DOF, RRRS) parallel robot is given to demonstrate the effectiveness of the base and tool calibration algorithm. As shown in the kinematic diagram in Fig. 1, the nominal kinematic transformations from the robot world frame to robot base frame and from the mobile platform frame to the tool frame are listed in Table II. The units of the kinematic parameters are in radians and millimeters. In order to verify the robustness of the proposed algorithm, the pose of $T_{B0,B}$ is specially arranged. Such an arrangement will be a singular configuration for the closed-form method.[8] In this example, we first simulate the calibration process under an ideal experimental condition without measurement noise. To obtain the actual tool frame poses, the following procedures are employed:

1. Assign kinematic errors at $T_{B0,B}$ and $T_{A,E}$ by introducing $\delta t'_{B0,B}$ and $\delta t'_{A,E}$, respectively (listed in Table I);
2. Find the actual poses of $T_{B0,B}$ and $T_{A,E}$ such that

Table I. Preset and Identified Kinematic Errors.

	Preset errors	Identified errors
$\delta t_{B0,B}$	(20, 20, 20, 0.2, 0.2, 0.2)^T	(20, 20, 20, 0.2, 0.2, 0.2)^T
$\delta t_{B0,B}$	$(-25, -25, -25, -0.25, -0.25, -0.25)^T$	$(-25, -25, -25 -0.25, -0.25, -0.25)^T$

https://doi.org/10.1017/S0263574702004101 Published online by Cambridge University Press

Table II. Nominal and Calibrated $T_{B0,B}$ and $T_{A,E}$.

	Nominal	Calibrated
$T_{B0,B}$	$\begin{bmatrix} -1 & 0 & 0 & 0 \\ 0 & 0 & 1 & 0 \\ 0 & 1 & 0 & 0 \\ 0 & 0 & 0 & 1 \end{bmatrix}$	$\begin{bmatrix} -0.9604 & 0.2158 & -0.1762 & 20 \\ -0.2158 & -0.1762 & 0.9604 & 20 \\ 0.1762 & 0.9064 & 0.2158 & 20 \\ 0 & 0 & 0 & 1 \end{bmatrix}$
$T_{A,E}$	$\begin{bmatrix} 1 & 0 & 0 & 0 \\ 0 & 1 & 0 & 0 \\ 0 & 0 & 1 & 100 \\ 0 & 0 & 0 & 1 \end{bmatrix}$	$\begin{bmatrix} 0.9385 & 0.2730 & -0.2115 & -46.150 \\ -0.2115 & 0.9385 & 0.2730 & 2.303 \\ 0.2730 & -0.2115 & 0.9385 & 68.847 \\ 0 & 0 & 0 & 1 \end{bmatrix}$

$$T_{B0,B} = e^{\delta\hat{\mathrm{t}}'_{B0,B}} T_{B0,B}$$

$$T_{A,E} = e^{\delta\hat{\mathrm{t}}'_{A,E}} T_{A,E}$$

3. Calculate the actual end-effector frame poses at different robot postures

$$T^a_{B0,E}(q) = T^a_{B0,B}\, T_{B,A}(q) T^a_{A,E}$$

Here the number of measured poses are set to 3 which is the necessary condition (lower bond) for identifying the kinematic errors[8] with perfect measurement data. The three given mobile platform poses $T_{B,A}(q)$ are listed in Table III). The success of the calibration simulation can be deduced from Table I, where all the preset kinematic errors are fully recovered although the preset kinematic errors are significantly large. A further re-enforcement of the calibration results is from Fig. 4, both the quantified orientation and position deviations, as in Equations (28) and (29), are driven from the initial magnitude of 160.450 mm and

Table III. Three given mobile platform poses $T_{B,A(q)}$.

Posture	$T_{B,A}(q)$
1	$\begin{bmatrix} 0.5964 & -0.6385 & 0.4864 & -117.155 \\ 0.8001 & 0.5217 & -0.2962 & 216.306 \\ -0.0647 & 0.5658 & 0.8220 & 445.614 \\ 0 & 0 & 0 & 1 \end{bmatrix}$
2	$\begin{bmatrix} 0.6219 & -0.7604 & 0.1873 & -226.347 \\ 0.7372 & 0.6491 & 0.1875 & -57.298 \\ -0.2642 & 0.0215 & 0.9642 & 571.754 \\ 0 & 0 & 0 & 1 \end{bmatrix}$
3	$\begin{bmatrix} 0.7082 & -0.7013 & -0.0811 & 126.003 \\ 0.4699 & 0.5540 & -0.6872 & -120.154 \\ 0.5268 & 0.4486 & 0.7220 & 421.954 \\ 0 & 0 & 0 & 1 \end{bmatrix}$

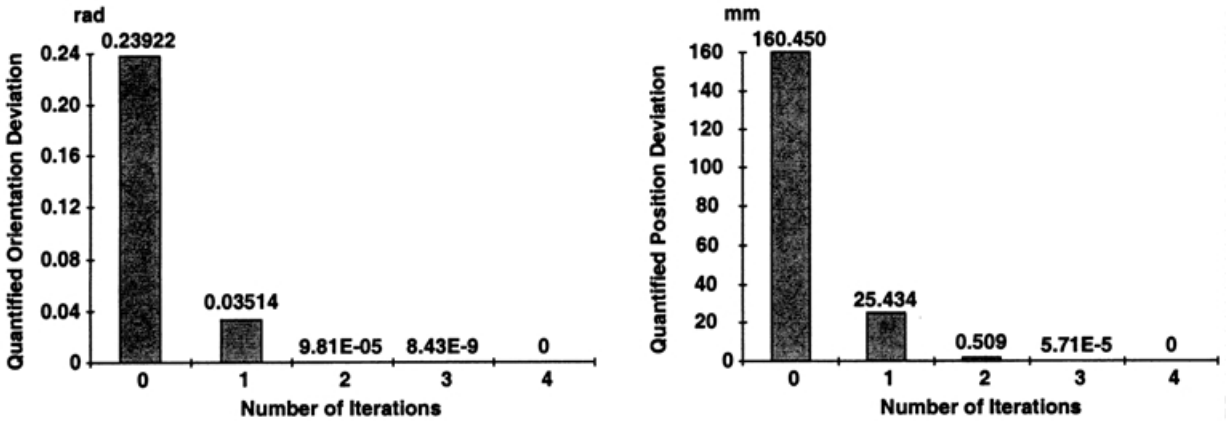


Fig. 4. Calibration Convergence.

https://doi.org/10.1017/S0263574702004101 Published online by Cambridge University Press

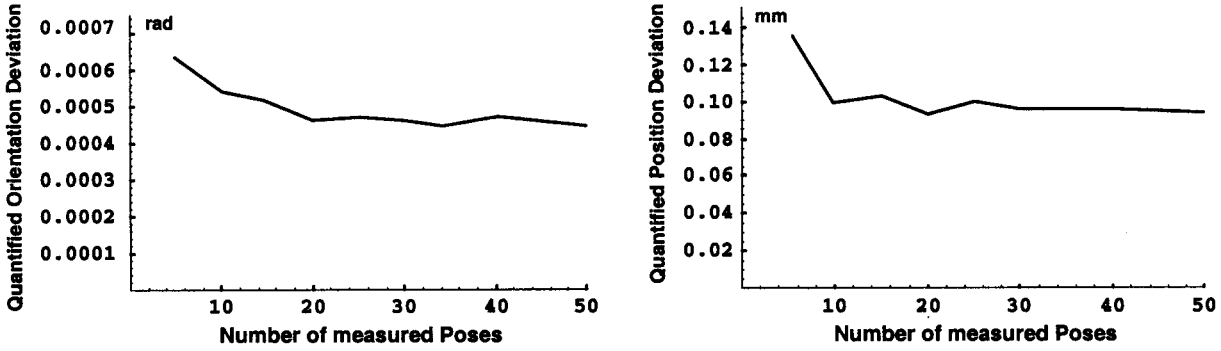


Fig. 5. Quantified deviation versus number of measurement postures.

0.2391 radian to values approximately zero with three to four iterations.

However, If the measurement noise exists, more measured end-effector poses will be considered. In the same example, we finally illustrate the effect of the measurement noise and robot repeatability on the calibration result. Form the viewpoint of computer simulation, both of the measurement noise and robot repeatability can be simulated in a uniform way by adding uniformly distributed noise on each of the actual (measured) end-effector's poses. The resulting actual endeffector's poses $T^{a*}_{B0,E}$ can be given by

$$T^{a*}_{B0,E} = e^{\hat{\delta}^*_{B0,E}} T^{a}_{B0,E} \tag{30}$$

where $\delta^* t_{B0,E} = (\delta x^*, \delta y^*, \delta z^*, \delta\alpha^*_x, \delta\beta^*_y, \delta\gamma^*_z)^T$ represents the noise injected. Here δx^*, δy^*, and $\delta z^* \in \mathbf{U}[-0.1, 0.1]$ mm; $\delta\alpha^*_x$, $\delta\beta^*_y$ and $\delta\gamma^*_z \in \mathbf{U}[-0.0005, 0.0005]$ rad.

Extensive simulations have been done to study the effect of the measurement noise and robot repeatability on the calibration results. In each simulation, two groups of 50 simulated end-effector's poses are employed. One group is used to calibrate the robot, while the other group is used to verify the result of the calibration, i.e. to derive the quantified orientation and position deviations. From these simulations, it can be found that the calibrated initial poses of the module frames and the quantified orientation and position deviations become stable when the number of poses used for calibration is greater than 20. A typical simulation result is given in Fig. 5, in which the stable quantified orientation and position deviations are in the same order of magnitude as that of the injected noise.

5. CONCLUSIONS

The concept of base and tool calibration is to improve the absolute positioning accuracy of a parallel robot by using external measuring equipment. Since it will be conducted after the parallel robot is self-calibrated, only the kinematic errors in the fixed transformations from the robot world frame to robot base frame and from the mobile platform frame to the tool frame need to be identified. Using the mathematical tools from differential geometry and group theory, a simultaneous base and tool calibration algorithm is developed for the self-calibrated parallel robots. Such a calibration model has a simple linear form, and an iterative least-square algorithm is employed to identify the error parameters. The simulation example on the end-effector calibration of a 6-DOF (RRRS) modular parallel robot shows that all of the preset errors are fully recovered within three to four iterations. In the presence of the measurement noise, the algorithm can also robustly identify the kinematic errors.

Acknowledgments

This work is funded by Gintic Institute of Manufacturing Technology, Singapore, under collaborative research project grant U-97-A006 and the Nanyang Technological University, Singapore, under Applied Research Grant RG29/99.

References

1. G. Yang, I. M. Chen, W. K. Lim and S. H. Yeo, "Design and kinematic analysis of modular reconfigurable parallel robots," *Proceedings of IEEE Conference on Robotics and Automation*, Detroit, USA (May, 1999) pp. 2501–2506.
2. H. Zhuang, "Self-calibration of parallel mechanisms with a case study on stewart platform," *IEEE Transactions on Robotics and Automation* **13**(3), 387–397 (1997).
3. H. Zhuang and L. Liu, "Self calibration of a class of parallel manipulators," *Proceedings of IEEE Conference on Robotics and Automation*, Minneapolis, USA. 994–999 (April, 1996).
4. D. J. Bennett and J. M. Hollerbach, "Autonomous calibration of single-loop closed kinematic chains formed by manipulators with passive endpoint constraints," *IEEE Transactions on Robotics and Automation* **7**(5), 597–606 (1991).
5. C. W. Wampler, J. M. Hollerbach and T. Arai, "An implicit loop method for kinematic calibration and its application to closed-chain mechanisms," *IEEE Transactions on Robotics and Automation* **11**(5), 710–724 (1995).
6. A. Nahvi, J. M. Hollerbach and V. Hayward, "Calibration of a parallel robot using multiple kinematic closed loops," *Proceedings of IEEE Conference on Robotics and Automation* 407–412 (1994).
7. G. Yang, I. M. Chen, W. K. Lim and S. H. Yeo, "Self-calibration of three-legged modular reconfigurable parallel robots based on leg-end distance errors," *Robotica* **19**, Part 2, 187–198 (2001) .
8. H. Zhuang and Z. S. Roth, "Simultaneous robot/word abd tool/flange calibration by solving homogeneous transformation equations of the form AX=BY," *IEEE Transactions on Robotics and Automation* **10**(4), 549–554 (1994).
9. F. C. Park and B. J. Martin, "Robot sensor calibration: Solving AX=XB on the Euclidean Group," *IEEE Transactions on Robotics and Automation* **10**(5), 717–721 (1994).
10. F. Dornaika and R. Horaud, "Simultaneous robot-world and hand-eye calibration," *IEEE Transactions on Robotics and Automation* **14**(4), 617–623 (1998).
11. R. Brockett, "Robotic manipulators and the product of exponential formula," *International Symposium in Math.*

https://doi.org/10.1017/S0263574702004101 Published online by Cambridge University Press

Theory of Network and Systems, Beer Sheba, Israel, 120–129 (1983).
12. F. C. Park, "Computational aspect of manipulators via product of exponential formula for robot kinematics", *IEEE Transactions on Automatic Control* **39**(9), 643–647 (1994).
13. R. Murray, Z. Li and S. S. Sastry, *A Mathematical Introduction to Robotic Manipulation* (CRC Press, 1994).
14. G. Yang, "Kinematics, dynamics, calibration, and configuration optimization of modular reconfigurable robots," *PhD thesis* (Nanyang Technological University, Singapore, 1999).
15. R. P. Paul, *Robot Manipulators*: *Mathematics*, *Programming*, *and Control* (MIT Press, Cambridge, 1981).
16. B. W. Mooring, Z. S. Roth and M. R. Driels, *Fundamentals of Manipulator Calibration* (John Wiley and Sons, 1991).

https://doi.org/10.1017/S0263574702004101 Published online by Cambridge University Press